Acta Crystallographica Section D
Biological Crystallography
ISSN 0907-4449

Crystallization and X-ray diffraction analysis of insect-cell-derived IL-22

Ting Xu,[a,b] Naomi J. Logsdon[a] and Mark R. Walter[a,b]*

[a]Center for Biophysical Sciences and Engineering, University of Alabama at Birmingham, Birmingham, AL 35294, USA, and [b]Department of Microbiology, University of Alabama at Birmingham, Birmingham, AL 35294, USA

Correspondence e-mail: walter@uab.edu

Received 1 March 2004
Accepted 29 April 2004

Interleukin-22 is a potent mediator of cellular inflammatory responses. Crystals of interleukin-22 expressed in *Drosophila melanogaster* S2 cells (IL-22Dm) have been grown from polyethylene glycol solutions. To obtain crystals suitable for X-ray diffraction analysis required the separation of different IL-22Dm glycosylation variants and the inclusion of the detergent cetyltrimethylammonium bromide (CTAB) in the crystallization experiments. The crystals belong to space group $P2_1$, with unit-cell parameters a = 64.88, b = 62.23, c = 139.524 Å, β = 91.35°, and diffract X-rays to 2.6 Å resolution. The crystallographic asymmetric unit contains six IL-22Dm molecules, corresponding to a solvent content of approximately 49%.

1. Introduction

Interleukin-22 (IL-22) is a recently identified α-helical cytokine produced by activated T cells (Dumoutier, Louahed *et al.*, 2000; Xie *et al.*, 2000). The biological function of IL-22 is still being defined. However, several studies show that it plays an important role in inflammatory responses. In particular, IL-22 has been shown to up-regulate the production of early systemically circulated defense proteins (acute phase proteins) such as serum amyloid A, α1-chymotrypsin and haptoglobin in liver cells (Dumoutier, Van Roost *et al.*, 2000). IL-22 also up-regulates gene expression of pancreatitis-associated protein, PAP1, in acinar cells (Aggarwal *et al.*, 2001) and induces the production of reactive oxygen species (ROS) in B-cells (Wei *et al.*, 2003). IL-22 biological responses are mediated through a heterodimeric receptor complex consisting of the cell-surface receptor chains IL-22R1 and IL-10R2 (Dumoutier, Louahed *et al.*, 2000; Dumoutier, Van Roost *et al.*, 2000; Kotenko *et al.*, 2001; Xie *et al.*, 2000).

IL-22 is a member of the class-2 cytokine family, which includes IL-10, IL-19, IL-20, IL-24 and IL-26 (Fickenscher *et al.*, 2002; Pestka *et al.*, 2004; Walter, 2002). Class-2 cytokines share ~25% sequence identity and have a largely conserved IL-10 footprint sequence (Walter & Nagabhushan, 1995). The crystal structure of IL-22 produced in *Escherichia coli* (IL-22Ec) has been determined (Nagem *et al.*, 2002). IL-22Ec exists as an α-helical monomer that is structurally similar to IL-10 (Logsdon *et al.*, 2002). However, in contrast to IL-10, IL-22 expressed in eukaryotic cells is glycosylated at one or more of its three N-linked glycosylation sites [Asn-*X*-Ser/Thr (N*X*S/T), where *X* is any amino acid]. The IL-22Ec crystal structure reveals that the three asparagines (Asn54, Asn68 and Asn97) involved in N*X*S/T glycosylation sites are located on helix *A*, the *AB* loop and helix *C* of the structure.

To test the role of glycosylation in receptor binding, IL-22 was expressed in *Drosphila melanogaster S2* cells (IL-22Dm) that attach hexasaccharides to N*X*S/T glycosylation sites (Manneberg *et al.*, 1994). Surface plasmon resonance (SPR) analysis reveals that a soluble extracellular fragment of the IL-10R2 chain exhibits a tenfold increase in affinity for IL-22Dm (K_d = 100 μM) compared with IL-22Ec ($K_d \simeq$ 1 mM) or an insect-cell-expressed IL-22 mutant ($K_d \simeq$ 1 mM) where the N*X*S/T sites have been destroyed by mutagenesis (N. J. Logsdon & M. R. Walter, unpublished results). Here, we report the crystallization of IL-22Dm, which may lead to an understanding of the structural basis for N-linked carbohydrate in IL-10R2 receptor recognition.

2. Materials and methods

2.1. Expression and purification

Restriction enzymes were purchased from New England Biolabs. All PCR experiments were performed using Pfu polymerase (Stratagene). An IL-22 expression construct was created by amplifying IL-22 cDNA from the plasmid hILTIF/pCEP4 (Renauld). The N-terminus of IL-22 was modified to code for a six-histidine affinity tag followed by a factor Xa protease site. The amplified PCR product was cut and ligated into the pMT/V5-HisA

expression plasmid (Invitrogen) to form pAHF-IL-22.

Transfection and selection of *D. melanogaster* S2 cells with pAHF-IL-22 and the hygromycin-resistance vector (pCpHYGRO) were performed as suggested by the manufacturer (Invitrogen). Expression was induced at a cell density of 5×10^6 cells ml^{-1} by the addition of 200 m*M* Cu_2SO_4 (0.5 m*M* final concentration) and allowed to proceed for 4 d. Cells were removed by centrifugation and the expression medium was dialyzed into buffer consisting of 20 m*M* Tris–HCl pH 7.9, 0.5 *M* NaCl (buffer *A*) containing 5.0 m*M* imidazole. 1 l dialyzed medium was subsequently applied onto a 10 ml nickel-affinity column (Novagen). The protein was extensively washed in buffer *A* containing 20 m*M* imidizole and subsequently eluted with a 1 *M* imidizole step gradient. Eluted fractions containing IL-22Dm were dialyzed overnight into 20 m*M* Tris–HCl pH 8.0, 1 m*M* EDTA, 100 m*M* NaCl and 3 m*M* $CaCl_2$. The His tag was removed by overnight incubation of His-tagged IL-22Dm with factor Xa [1:50(*w*:*w*)]. The resulting digestion mixture was diluted tenfold with 20 m*M* Tris–HCl pH 8.0 and loaded onto a 1.6 ml Poros 20HQ column. Purified IL-22Dm was collected in the flowthrough and concentrated to 10 mg ml^{-1} using a Centriprep 10 (Amicon). Protein concentrations for all experiments were determined by UV absorbance at 280 nm using a calculated $\varepsilon^{0.1\%}$ value of 0.24.

2.2. Mass spectrometry

Native and deglycosylated IL-22Dm samples were analyzed by MALDI–TOF mass spectrometry (MS) on a Voyager Elite mass spectrometer (Perseptive Biosystems) operating in postive mode. Samples were mixed in a 1:10 ratio with sinapinic acid dissolved in 1:1 acetonitrile:0.1% TFA. Enzymatic deglycosylation experiments on IL-22Dm were performed with PNGaseF (New England Biolabs) under native conditions. IL-22Dm samples (0.5 mg ml^{-1}) in 20 m*M* NaCl, 20 m*M* Tris–HCl pH 8.0 were incubated overnight with dilutions of PNGaseF ranging from 0–500 times the supplier's recommended enzyme concentration required for complete cutting of denatured proteins.

2.3. Crystallization

All crystallization experiments employed the hanging-drop method. Crystallization drops consisted of 1 µl of IL-22Dm or IL-22Dm cation-exchange fractions at 10 mg ml^{-1} in 20 m*M* Tris–HCl pH 8.0 combined with 1 µl of a solution consisting of 100 m*M* trisodium citrate pH 6.0, 0.2 *M* ammonium acetate, 1.4 m*M* CTAB and 20% PEG 4000. The drops were equilibrated at 310 K against a well solution consisting of 0.1 *M* trisodium citrate pH 6.0, 20% PEG 4000. All buffers and precipitant solutions were warmed to 310 K prior to setting up the experiments. Despite numerous attempts at optimization, the conditions described yielded the highest quality crystals obtainable for the heterogeneous IL-22Dm protein and the cation-exchange fractions *F*6–*F*9 described in §3.1 (see Figs. 1 and 2).

Table 1
IL-22Dm glycosylation variants identified by MALDI–TOF MS.

The peak number corresponds to the qualitative estimated abundance (determined by SDS–PAGE and MS) of the variant, with 1 being the most abundant.

Peak No.	IL-22Dm glycosylation variant	No. glycans	Mass	
			Observed	Predicted
1	IL-22 + 2-($GlcNAc_2Man_3Fuc$)-1-($GlcNAc_2Man_3$)	3	19722.8	19719
2	IL-22 + 1-($GlcNAc_2Man_3Fuc$)-2-($GlcNAc_2Man_3$)	3	19575.2	19572
3	IL-22 + 1-($GlcNAc_2Man_3Fuc$)-1-($GlcNAc_2Man_3$)	2	18684.6	18680
4	IL-22 + 2-($GlcNAc_2Man_3Fuc$)	2	18832.9	18827
5	IL-22 + 1-($GlcNAc_2Man_3Fuc$)	1	17792.1	17788
6	IL-22	0	16749.0	16749

3. Results and discussion

3.1. Characterization of IL-22Dm

SDS–PAGE analysis of purified IL-22Dm revealed three bands between ∼16 and ∼20 kDa that are consistent with the presence of N-linked glycosylation at each of the three N*X*S/T sites (Fig. 1, lane *a*). To confirm this hypothesis, IL-22Dm was enzymatically deglycosylated with PNGaseF, which cleaves the glycosydic bond and converts the N-linked asparagine residue into an aspartate. SDS–PAGE analysis of the PNGaseF-treated samples reveals four protein bands separated by ∼1 kDa, corresponding to IL-22Dm species with three, two, one and no N-linked carbohydrate species, respectively (Fig. 1, lanes *b*–*d*). To confirm this analysis, mass spectrometry was performed on purified IL-22Dm (Fig. 1, lane *a*) and PNGaseF-treated samples (Fig. 1, lanes *b*–*d*). Mass-spectroscopic analysis of purified IL-22Dm (Fig. 1, lane *a*) identified six peaks with molecular massess of 19 722.8 (peak 1), 19 575.2 (peak 2), 18 684.6 (peak 3), 18 832.9 (peak 4), 17 792.1 (peak 5) and 16 749.0 (peak 6). These same peaks were observed in different ratios in the IL-22Dm sample treated with 0.06 units of PNGaseF (Fig. 1, lane *b*). Only peak 6 and an additional peak with a mass of 17 639.2 were observed in the IL-22Dm samples treated with 6 and 300 units of PNGaseF (Fig. 1, lanes *c* and *d*). The 147 Da difference between peaks 1 and 2 and peaks 3 and 4 cannot be resolved by SDS–PAGE, resulting in the four gel bands observed in Fig. 1, which correspond to the number of N-linked glycans (0–3) attached to IL-22Dm variants.

Using the expected weights of the carbohydrate moieties and the IL-22 polypeptide chain without N-linked carbohydrate (16 749 Da), the glycosylation state of IL-22Dm was further defined (Table 1). Previous characterization of insect-cell glycosylation has shown the most common N-linked glycan is a hexasaccharide with a molecular weight of 1039 Da, which consists of two *N*-acetyl glucosamines (GlcNAc, 203 Da), three mannose residues (Man,

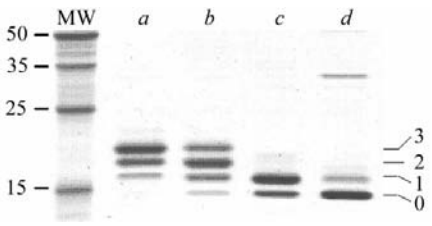

Figure 1
SDS–PAGE gel of IL-22Dm treated with PNGaseF. Lanes *a*–*d* correspond to IL-22Dm protein treated with 0 (*a*), 0.06 (*b*), 6 (*c*) and 300 (*d*) units of PNGaseF. Gel bands are labelled according to the number of N-linked glycans attached to IL-22. The band at ∼35 kDa in lane *d* corresponds to PNGaseF.

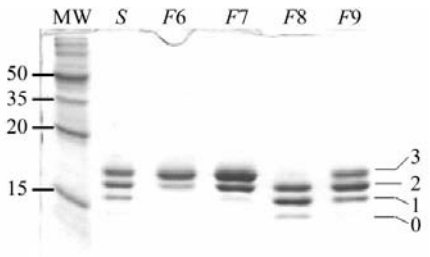

Figure 2
SDS–PAGE gel of cation-exchange-purified IL-22Dm glycosylation variants. Lane *S* corresponds to the IL-22Dm starting material. Lanes *F*6–*F*9 correspond to IL-22Dm cation-exchange fractions 6–9. Gel bands are labelled according to the number of N-linked glycans attached to IL-22.

162 Da) and one fucose moiety (Fuc, 147 Da) (Manneberg *et al.*, 1994). Analysis of the MS data reveals that heterogeneity in the glycans attached to IL-22Dm mostly arises from the presence or absence of a fucose moiety. For example, IL-22Dm variants with three glycans attached to the N*X*S/T sites (peak 1 and 2) contain two hexasaccharides ($GlcNAc_2Man_3Fuc$) and one pentasaccharide ($GlcNAc_2Man_3$) or one hexasaccharide and two pentasaccharides (Table 1). The combination of SDS–PAGE and MS data clearly show that IL-22Dm glycosylation variants containing three or two glycans (peaks 1–4) are the predominant forms of IL-22 expressed in *D. melanogaster* S2 cells. Although our studies clearly define the number and type of glycans attached to IL-22Dm, we cannot identify which glycan is attached at a specific N*X*S/T site.

3.2. Crystallization

Initial crystal screening experiments were performed using IL-22Dm purified by nickel-affinity and anion-exchange chromatography (Fig. 1, lane *a*; Fig. 2, lane *S*). As described above, SDS–PAGE and MS analysis revealed that the protein preparation was heterogeneous owing to the presence of N-linked glycosylation attached to each of the three N*X*S/T glycosylation sites. Despite the chemical heterogeneity of IL-22Dm, crystallization screens performed with the Crystal Screen I kit (Hampton Research) at 298 and 277 K yielded small crystals in conditions No. 9 and 40 at 298 K. Condition No. 9 contained ∼5 × ∼15 µm needles and ∼30 µm crystalline aggregates grew in condition No. 40. Refinement of the initial conditions revealed that 0.7 m*M* cetyltrimethylammonium bromide (CTAB) improved the size of the crystals (∼0.1 mm), but the morphology actually became worse. Increasing the temperature of the crystallization experiments to 310 K resulted in a considerable improvement in morphology, but the size of the crystals was limited to approximately 50 µm on an edge and further optimization was not successful.

Marked enhancement in crystal size was only accomplished by additional purification of the IL-22Dm glycosylation variants into the four ion-exchange chromatography fractions (*F*6–*F*9) shown in Fig. 2. This was accomplished by dialysis of IL-22Dm into 20 m*M* NaCl, 20 m*M* PIPES pH 6.5 and subsequent loading of the material onto a 1.66 ml POROS HS20 column at a flow rate of 2 ml min^{-1}. Glycosylation variants were eluted with a 1 *M* NaCl gradient in 15 column volumes. Interestingly, the largest single crystals suitable for data collection could only be grown from IL-22Dm variants containing three or two N-linked glycans (fractions 6 and 7). IL-22Dm fractions containing one or two glycans (*F*8 and *F*9) did not yield crystals suitable for X-ray diffraction experiments (Fig. 3). Although fraction *F*9 contains some IL-22Dm with three and two N-linked glycans, as found in fractions *F*6 and *F*7, this material is not amenable to crystallization. Possible reasons for this are the contamination of the fractions with IL-22 glycosylation variants containing only one glycan or a shorter or different chemical composition of the glycans present on each asparagine residue as suggested by MS analysis. The best crystals of IL-22Dm were grown from the early eluting fraction 7 (Figs. 2 and 3).

Table 2
Data collection.

Values in parentheses are for the highest resolution shell.

Wavelength (Å)	1.255
Resolution (Å)	50–2.6 (2.69–2.60)
No. observations	108300
No. unique observations	32705 (2720)
Redundancy	3.3 (2.8)
Completeness (%)	94.5 (79.5)
$I/\sigma(I)$	21.3 (2.1)
R_{merge} (%)	0.051 (0.344)
Space group	$P2_1$
Unit-cell parameters	
a (Å)	64.88
b (Å)	62.23
c (Å)	139.52
β (°)	91.35

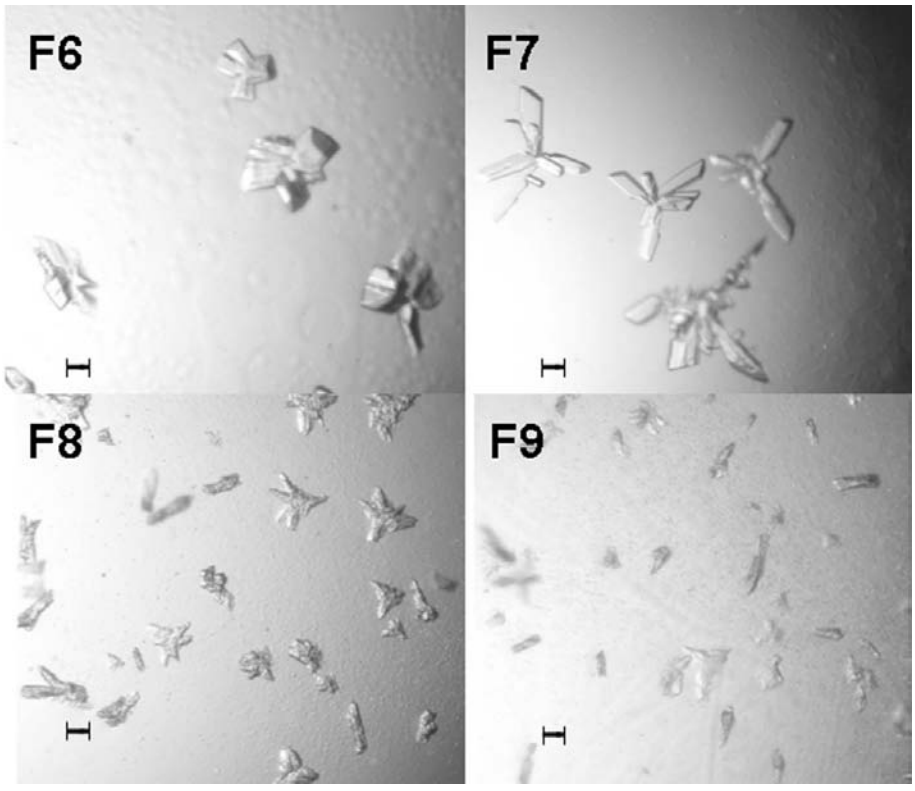

Figure 3
Crystals of IL-22Dm obtained with cation-exchange fractions 6–9 shown in Fig. 2. The measurement bar corresponds to 0.1 mm.

3.3. X-ray diffraction

Crystals of IL-22Dm were flash-cooled for low-temperature data collection in a nitrogen stream (100 K) following exchange of the drop solution with a solution of 0.1 *M* trisodium citrate pH 6.0, 0.2 *M* ammonium acetate and 29% PEG 4000. The cryosolution was pre-warmed to 310 K prior to transferring the crystal from the crystallization drop. Diffraction data were collected at the South Eastern Region Collaborative Access Team (SER-CAT) beamline ID-22 at the Advanced Photon Source, Argonne National Laboratory. Data were collected on a MAR 165 CCD detector using a wavelength of 1.25 Å, an oscillation range of 1° and an exposure time of 1 s, resulting in a complete 2.6 Å resolution data set. Reflection intensities were indexed, integrated and scaled using *HKL*2000 (Otwinowski & Minor, 1997). The *HKL*2000 indexing routine combined with the analysis of systematic absences identified the space group as $P2_1$, with unit-cell parameters $a = 64.88$, $b = 62.23$, $c = 139.52$ Å, $\beta = 91.35°$.

Data-collection statistics are shown in Table 2.

Since it is assumed that IL-22Dm crystals contain IL-22 molecules that contain two or three N-linked glycans, an average molecular weight of 19 204 Da was estimated from peaks 1–4 in Table 1. Calculations using this molecular weight resulted in three reasonable solvent estimates of 66% (V_M = 3.7 Å^3 Da^{-1}), 58% (V_M = 2.9 Å^3 Da^{-1}) and 49% (V_M = 2.4 Å^3 Da^{-1}), corresponding to four, five or six molecules in the asymmetric unit, respectively (Matthews, 1968). To distinguish between these choices, a self-rotation function (SRF) was performed with *AMoR*e using data in the resolution range 20–4 Å (Navaza, 1994). Excluding the origin peak, the three largest peaks in the SRF map correspond to three distinct non-crystallographic twofold axes. A non-crystallographic twofold axis was previously observed in the asymmetric unit of IL-22Ec crystals (Nagem *et al.*, 2002). Together, the data suggests IL-22Dm crystals contain six molecules of IL-22 comprised of three non-crystallographically related IL-22 dimers that pack in a yet unknown manner. Molecular replacement and refinement of the structure to confirm this hypothesis and elucidate the role of the N-linked carbohydrate in IL-22 structure and function are currently under way.

This work is supported by the NIH (grant AI47300). Use of the Advanced Photon Source was supported by the US Department of Energy, Office of Science, Office of Basic Energy Sciences under Contract No. W-31-109-Eng-38. We thank Landon Wilson for help with mass spectrometry and acknowledge equipment and partial operating costs are provided by grants S10RR11329 and P30CA-13148.

References

Aggarwal, S., Xie, M. H., Maruoka, M., Foster, J. & Gurney, A. L. (2001). *J. Interferon Cytokine Res.* **21**, 1047–1053.

Dumoutier, L., Louahed, J. & Renauld, J. C. (2000). *J. Immunol.* **164**, 1814–1819.

Dumoutier, L., Van Roost, E., Colau, D. & Renauld, J. C. (2000). *Proc. Natl Acad. Sci. USA*, **97**, 10144–10149.

Fickenscher, H., Hor, S., Kupers, H., Knappe, A., Wittmann, S. & Sticht, H. (2002). *Trends Immunol.* **23**, 89–96.

Kotenko, S. V., Izotova, L. S., Mirochnitchenko, O. V., Esterova, E., Dickensheets, H., Donnelly, R. P. & Pestka, S. (2001). *J. Biol. Chem.* **276**, 2725–2732.

Logsdon, N. J., Jones, B. C., Josephson, K., Cook, J. & Walter, M. R. (2002). *J. Interferon Cytokine Res.* **22**, 1099–1112.

Manneberg, M., Friedlein, A., Kurth, H., Lahm, H. W. & Fountoulakis, M. (1994). *Protein Sci.* **3**, 30–38.

Matthews, B. W. (1968). *J. Mol. Biol.* **33**, 491–497.

Nagem, R. A., Colau, D., Dumoutier, L., Renauld, J. C., Ogata, C. & Polikarpov, I. (2002). *Structure*, **10**, 1051–1062.

Navaza, J. (1994). *Acta Cryst.* A**50**, 157–163.

Otwinowski, Z. & Minor, W. (1997). *Methods Enzymol.* **276**, 307–326.

Pestka, S., Krause, C. D., Sarkar, D., Walter, M. R., Shi, Y. & Fisher, P. B. (2004). *Annu. Rev. Immunol.* **22**, 929–979.

Walter, M. R. (2002). *Immunol. Res.* **26**, 303–308.

Walter, M. R. & Nagabhushan, T. L. (1995). *Biochemistry*, **34**, 12118–12125.

Wei, C. C., Ho, T. W., Liang, W. G., Chen, G. Y. & Chang, M. S. (2003). *Genes Immun.* **4**, 204–211.

Xie, M. H., Aggarwal, S., Ho, W. H., Foster, J., Zhang, Z., Stinson, J., Wood, W. I., Goddard, A. D. & Gurney, A. L. (2000). *J. Biol. Chem.* **275**, 31335–31339.